ARTHRITIS & RHEUMATISM
Vol. 56, No. 11, November 2007, pp 3726–3737
DOI 10.1002/art.22976

The Aminobisphosphonate Risedronate Preserves Localized Mineral and Material Properties of Bone in the Presence of Glucocorticoids

Guive Balooch,[1] Wei Yao,[2] Joel W. Ager,[3] Mehdi Balooch,[4] Ravi K. Nalla,[3] Alexandra E. Porter,[5] Robert O. Ritchie,[3] and Nancy E. Lane[2]

Objective. **Glucocorticoids (GCs) alter bone strength such that patients receiving these medications have a high rate of fragility-related fractures. The purpose of this study was to assess whether concurrent treatment with GCs (prednisolone) and risedronate (an aminobisphosphonate) would prevent the reduction in bone strength induced by GCs, in a mouse model of GC-induced bone loss and in patients enrolled in a clinical study.**

Methods. **We evaluated mice treated with prednisolone pellets alone, GCs plus risedronate, or placebo alone and iliac crest biopsy specimens obtained from patients who were treated with GCs plus placebo or GCs plus risedronate for 1 year. We measured the mass, architecture, and physical and material properties of bone (subject to therapeutic treatments) at nanoscale to macroscopic dimensions, using synchrotron x-ray tomography, elastic modulus mapping, transmission electron microscopy, and small-angle x-ray scattering techniques.**

Results. **GC treatment reduced trabecular bone mass, microarchitecture, and the degree of bone mineralization and elastic modulus within the trabeculae. Concurrent treatment with GCs and risedronate prevented the deterioration of trabecular bone architecture, reduced the degree of mineralization, and preserved elastic modulus within the trabeculae, in both mouse and human bone. In addition, treatment with risedronate plus GCs in mice appeared to preserve bone crystal orientation, compared with treatment with GCs alone.**

Conclusion. **Risedronate prevented the localized changes in mineral and material properties of bone induced by GCs, which may ultimately improve bone strength.**

Glucocorticoids (GCs) are frequently prescribed for the treatment of many noninfectious inflammatory conditions, including arthritis, pulmonary diseases, and skin diseases. GCs are potent antiinflammatory agents, and long-term use results in several adverse side effects, the most common of which is osteoporosis (1–3). GC-induced osteoporosis (GIOP) is caused by suppression of bone formation and enhancement of bone resorption; the resulting changes in bone architecture lead to increased bone fragility (1–3). Bisphosphonates, which act as antiresorptive agents, are widely used for the treatment of metabolic bone diseases such as GIOP and estrogen deficiency–related bone loss (4–9). It is known that bisphosphonate therapy can reduce the risk of new vertebral fracture in patients with estrogen deficiency and in those with GIOP; however, the mechanism by which such treatment increases bone strength and reduces vertebral fracture risk remains unclear (5–7).

At present, the changes in bone mass and structure, as measured by standard clinical techniques in prior studies of concurrent treatment with bisphosphonates and GCs, explain very little of the dramatic reduction in fracture risk (5–7,10). For example, risedronate and other aminobisphosphonates have been shown to reduce the incident vertebral fracture risk after 1 year in patients treated with GCs, even though the bone mineral density (BMD) of

Supported by NIH grants R01-AR-043052-07, R01-DK-46661-10, and 1K24-AR-48841-03, and a Procter & Gamble research grant. Drs. G. Balooch, Ager, Nalla, and Ritchie's work was supported by the Laboratory Directed Research and Development Program of Lawrence Berkeley National Laboratory under contract no. DE-AC02-05CH11231 from the US Department of Energy. This contract also provides support for the Advanced Light Source, a division of Lawrence Berkeley National Laboratory.

[1]Guive Balooch, PhD: Lawrence Berkeley National Laboratory, Berkeley, California, and University of California, San Francisco; [2]Wei Yao, MD, Nancy E. Lane, MD: Center for Healthy Aging, University of California at Davis, Sacramento; [3]Joel W. Ager, PhD, Ravi K. Nalla, PhD, Robert O. Ritchie, MA, PhD, ScD: Lawrence Berkeley National Laboratory, Berkeley, California; [4]Mehdi Balooch, PhD: University of California, San Francisco; [5]Alexandra E. Porter, PhD: Nanoscience Centre, Cambridge University, Cambridge, UK.

Address correspondence and reprint requests to Nancy E. Lane, MD, University of California at Davis, Department of Medicine, 4800 Second Avenue, Suite 2600, Sacramento, CA 95817. E-mail: nelane@ucdavis.edu.

Submitted for publication February 2, 2007; accepted in revised form July 20, 2007.

the lumbar spine increased by <1–3% during this treatment period (5,9,11,12). These data suggest that, in addition to regulating whole bone density, the aminobisphosphonates may be regulating other local bone matrix properties that can ultimately influence bone fragility.

A known mechanism by which aminobisphosphonates influence bone strength is through inhibition of osteoclast-mediated bone resorption, which results in a reduction in bone turnover. Aminobisphosphonates act directly on osteoclasts to inhibit isoprenoid biosynthesis and protein prenylation (13,14). In addition, they also activate caspase cleavage of Mst1 kinase (15), ultimately leading to osteoclast apoptosis and a reduction in bone resorption (16–18). Aminobisphosphonates have also been shown to bind and inhibit hydroxyapatite crystal growth (19) and to be more active in promoting surface hydroxyapatite nucleation compared with other known bisphosphonates (19). Given the role of aminobisphosphonates in binding and regulating hydroxyapatite nucleation and osteoblast and osteoclast activity, it is reasonable to suggest that they may be involved in regulating the local mechanical properties of the bone matrix.

In this study, we used several ultrastructural and microstructural evaluation techniques to determine whether concurrent treatment with GCs (prednisolone) and risedronate would change the mechanical properties of bone (determined at both nano/micro and macro dimensions) and the degree of bone mineralization (DBM), as compared with GC treatment alone. To test this hypothesis, we evaluated trabecular bone from mice treated with GCs alone, GC plus risedronate, or placebo alone, and human iliac crest biopsy specimens obtained from patients treated with GCs plus placebo or GCs plus risedronate. We found that, in addition to increasing whole bone strength, treatment with risedronate in the presence of GCs reduced the degree of deterioration of bone mineralization and local mechanical properties in mouse and human trabecular bone. These results suggest that concurrent treatment with risedronate in GC-treated mice and humans maintains localized nanomechanical properties and mineralization, enabling these bones to better resist fracture.

MATERIALS AND METHODS

Animals and experimental procedures. Six-month-old male Swiss-Webster mice were obtained from Charles River (San Jose, CA). The mice were maintained on commercial rodent chow (22/5 Rodent Diet; Harlan Teklad, Madison, WI), available ad libitum, with 0.95% calcium and 0.67% phosphate. Mice were housed in a room that was maintained at 21°C with a 12-hour light/dark cycle. The mice were randomized by body weight into 3 groups of 8–15 animals each. Slow-release pellets (Innovative Research of America, Sarasota, FL) containing placebo (group 1, n = 15) or 1.5 mg/kg/day of prednisolone (group 2, n = 15) were administered for 21 days by subcutaneous implantation (18,20). Risedronate, at a dosage of 5 μg/kg/day, 5 times per week, was administered to GC-treated animals (group 3, n = 8) (21). The protocol was approved by the University of California Davis Animal Experiment Committee.

Iliac crest biopsy specimens. The iliac crest biopsy specimens were obtained from individuals enrolled in a GC treatment study. Study subjects consented to undergo an iliac crest biopsy at the time of study initiation (baseline) and after 1 year. The biopsy specimens were processed and provided to our research group in methylmethacrylate. Specimens were randomly selected from the placebo group (n = 3 paired samples, at baseline and after 1 year of treatment) and the group receiving risedronate (n = 3 paired samples). (For additional information about the clinical study that used these biopsy specimens, see ref. 9.) All protocols were approved by the individual institutional review boards, prior to obtaining iliac crest biopsy samples.

Biochemical markers. Urinary levels of deoxypyridinoline crosslinks and creatinine (DPD) were analyzed in duplicate, using enzyme-linked immunoabsorbent (ELISA) kits from Quidel (Mountain View, CA). Serum levels of osteocalcin, tartrate-resistant acid phosphatase 5b (TRAP5b), and RANKL were measured using mouse sandwich ELISA kits from Biomedical Technologies (Stoughton, MA), SBA Sciences (Fountain Hills, AZ), and ALPCO Diagnostics (Salem, NH), respectively. The manufacturers' protocols were followed, and all samples were assayed in duplicate. A standard curve was generated from each kit, and the absolute concentrations were extrapolated from the standard curve. The coefficients of variations for interassay and intraassay measurements were <10% for all assays and were similar to the manufacturer's references (20,21).

Microfocal computed tomography (micro-CT). The fifth lumbar vertebral body from each mouse was scanned using a desktop micro-CT system (μCT 40; Scanco Medical, Bassersdorf, Switzerland), with an isotropic resolution of 10.5 μm for the vertebral body in all 3 spatial dimensions (20,21). The scans were initiated in the sagittal plane of the vertebral body and covered the entire cortical and trabecular bone of the vertebral body. Secondary spongiosa was consistently selected for evaluation (20–22). Three-dimensional (3-D) trabecular structural parameters were measured directly, as previously described (20,21,23).

Bone histomorphometric analysis. After micro-CT analysis, the fifth lumbar vertebral bodies were dehydrated in ethanol, embedded undecalcified in methylmethacrylate, and sectioned longitudinally with a Leica/Jung 2255 microtome (Leica Microsystems, Bannockburn, IL) at 4-μm and 8-μm thick sections. Bone histomorphometry was performed using a semiautomatic image analysis system (Bioquant Image Analysis, Nashville, TN) linked to a microscope equipped with transmitted and fluorescence light.

A counting window, allowing measurement of all trabecular bone and bone marrow within the growth plate and cortex, was created for the histomorphometric analysis. Measurements included osteoclast surface, single-labeled perimeter, double-labeled perimeter, and interlabel width. These indices were used to measure the mineralizing surface, the percentage of osteoclast surface, the mineral apposition rate, and the surface-based bone formation rate, as previously reported (24,25).

Elastic modulus mapping. Quantitative elastic modulus measurements at nanoscale dimensions were acquired using direct-force modulation in a modified atomic-force microscope equipped with a nanoindenter (26). By applying a small sinusoidally modulated force (~3 μN) to the transducer of the nanoindenter, elastic modulus mapping measuring 256 × 256 pixels of modulus values with a 15-nm step size was obtained without plastically deforming the material. The measurements and the tip contact radius were calibrated using a standard quartz sample with a known elastic modulus. To prepare the specimens for such measurements, the methylmethacrylate-embedded lumbar vertebral bodies that had been used to generate sections for bone histomorphometric analysis were further polished with different diamond pastes, from 10 μm to 0.1 μm in diameter, to obtain smooth surfaces. Measurements were performed on 1 randomly selected vertebral specimen per treatment group and ~4–5 different trabeculae from each sample (20).

Transmission electron microscopy. Bone samples from the fourth lumbar vertebrae (n = 3 per group) were prepared by first treating with 3 changes of 100% ethanol over 15 minutes to dehydrate them and 3 changes of acetonitrile (a transitional solvent) over 1 hour. The beams were then infiltrated with Spurr's resin (Agar Scientific, Essex, UK) over a period of several days. Precasting an ~200-μm layer of Spurr's resin into the truncated beam capsules before adding the bone section facilitated initial sectioning of the blocks. Sections (50–70 nm thick) were then cut onto distilled water with an ultramicrotome (Boeckeler Instruments, Tucson, AZ) using a 55° diamond knife. Sections were collected immediately on lacey carbon 300 mesh copper grids and dried for 1 hour at 37°C. Low-magnification bright-field imaging was performed using a JEOL 3010 microscope (JEOL, Peabody, MA) (27,28).

Small-angle x-ray scattering (SAXS). SAXS data were collected with a Bruker Nanostar spectrometer (Bruker Instruments, Ettlingen, Germany) using Cu Kα radiation (γ = 1.54Å). The fifth lumbar vertebral body samples (n = 2 from each group) were thinned to ~100 μm by polishing and oriented with the long axis of the bone parallel to the q_x direction. The sample-to-camera distance was 104.65 mm, and 2-D data were collected with a pressurized xenon gas detector (Bruker HiStar). A typical collection time was 2 hours. The instrument was calibrated using a silver behenate standard. The sampled q range was 0.1 $nm^{-1} < q_x, q_y < 2.1\ nm^{-1}$, and 3 scattering images were obtained from each sample at different locations. Analytic techniques developed by Fratzl and coworkers (29) were used to calculate the average thickness T and the average orientation of the crystallite along the long axis of the bone (0–100%, where random orientation is 0%).

X-ray tomography (XTM). XTM studies were used to assess the degree of bone mineralization. The procedures were based on those previously described by our group (23). The proximal tibial metaphyses (n = 4 per group) of mouse bone and human iliac crest biopsy specimens (n = 3 paired specimens from each treatment group) were scanned to determine the degree of mineralization. The proximal tibial metaphysis was scanned to assess the DBM, because we observed the correlation with the cancellous bone volume of the lumbar vertebrae to be >80% in these mice. X-ray imaging was performed at the Advanced Light Source synchrotron on beamline (8.3.2) at the Lawrence Berkeley National Laboratory, by obtaining 2-D radiographs as the specimens were rotated through 180° in 0.5° increments. The radiographs were reconstructed into 1,000 slices by Fourier-filtered back projection with an 11.7-μm resolution. The attenuation coefficient (mm^{-1}) of each pixel is represented by the false colors and relates directly to bone mineral concentration. In addition, the bone surface to bone volume ratio (BV/TV) was calculated, using procedures described previously (21,23).

Biomechanical testing. Biomechanical testing was achieved by compression testing of the sixth lumbar vertebrae at ambient temperature. Stiffness was assessed from the initial (elastic) slope of the load-displacement curve. The cross-sectional dimensions of length and height were measured and used to determine the macroscopic compression modulus (20,30). The compression strength, which is a relative measure of the fracture resistance of the bone, was determined from the maximum load (P_{max}) and cross-sectional dimensions. Measurements were based on load-displacement curves, which were recorded at a crosshead speed of 0.01 mm/second, using a mechanical test frame (ELF 3200; EnduraTEC, Minnetonka, MN).

Statistical analysis. The group means and SDs were calculated for all outcome variables. To determine significant differences between groups, the Kruskal-Wallis nonparametric test was used. When Kruskal-Wallis testing showed overall

Table 1. Trabecular bone structure and turnover variables, according to micro-CT and histomorphometry results from the fifth lumbar vertebral body*

Variable	Treatment group		
	Placebo	GCs alone	GCs plus risedronate
Trabecular bone volume, %	42.5 ± 5.2	37.0 ± 3.4†	49.3 ± 17.0
Trabecular connectivity, mm^3	89.6 ± 24.1	78.4 ± 40.0	79.6 ± 21.7
Trabecular number, mm	5.1 ± 0.9	3.9 ± 1.0‡	4.0 ± 1.0
Trabecular thickness, μm	84.5 ± 6.7	83.5 ± 15.1	115.8 ± 32.4
Osteoclast surface, %	1.46 ± 0.27	3.09 ± 0.72†	1.13 ± 0.19
Mineral apposition rate, μm/day	1.43 ± 0.26	0.88 ± 0.32‡	0.77 ± 0.31
Bone formation rate/bone surface, $\mu m^3/\mu m^2$/day	0.21 ± 0.07	0.04 ± 0.01‡	0.02 ± 0.02

* Values are the mean ± SD. Micro-CT = microfocal computed tomography; GCs = glucocorticoids.
† $P < 0.05$ versus placebo and GCs plus risendronate.
‡ $P < 0.05$ versus placebo.

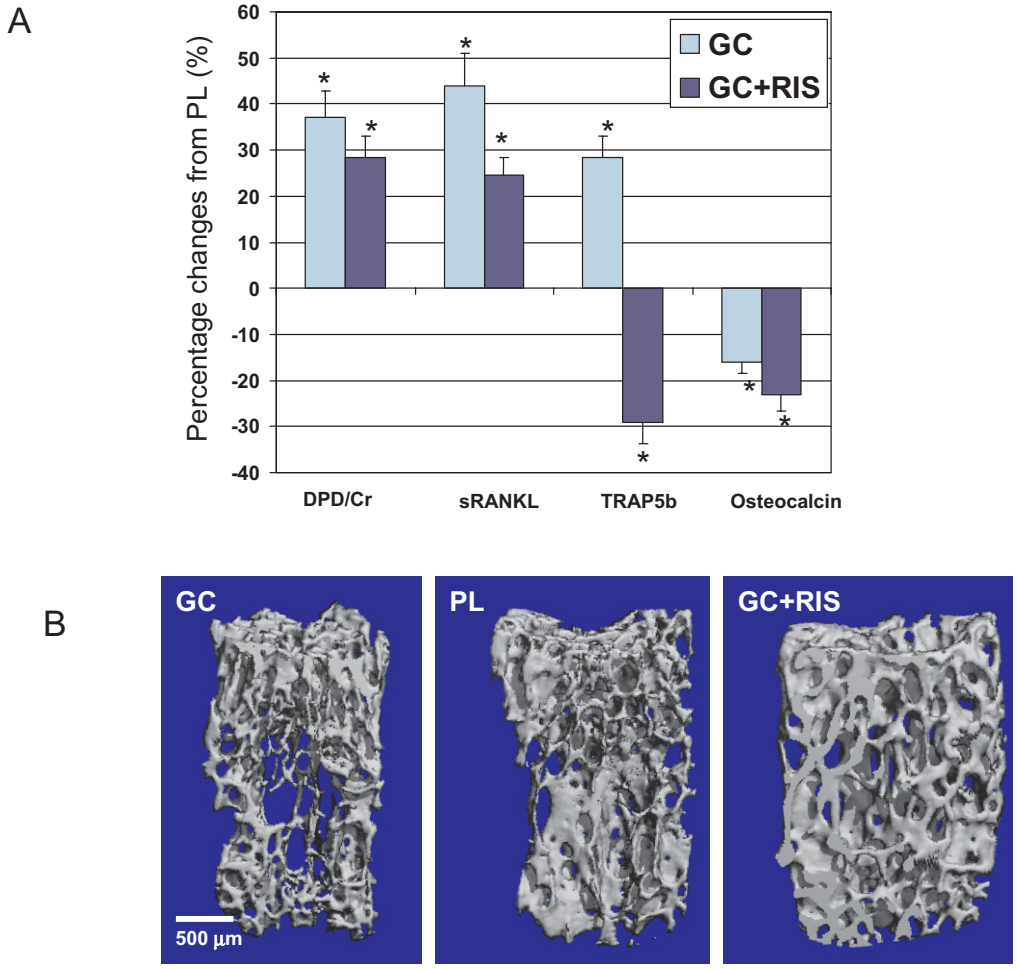

Figure 1. Bone turnover, trabecular mass, and architecture. **A,** In the mouse study, the levels of bone turnover markers (deoxypyridinoline crosslinks and creatinine [DPD], soluble RANKL [sRANKL], and tartrate-resistant acid phosphatase 5b [TRAP5b]) were significantly increased with glucocorticoid (GC) treatment and significantly decreased with GC plus risedronate (RIS) treatment compared with placebo (PL) treatment. The level of osteocalcin, another marker of bone turnover, decreased with both active treatments compared with placebo. Bars show the mean and SD. $* = P < 0.05$. **B,** Representative 3-dimensional sample from each treatment group, from the microfocal computed tomography evaluation of the trabecular bone microstructure of the fifth lumbar vertebral body. Treatment with GCs reduced trabecular bone mass and microarchitecture, and the preventive effects of treatment with GCs plus risedronate were similar to those of placebo.

significant differences between all groups, Ryan's post hoc test was applied to identify groups that were significantly different (SPSS version 12; SPSS, Chicago, IL). *P* values less than 0.05 were considered significant.

RESULTS

Prevention of GC-induced trabecular bone loss by risedronate. In mice that were treated with GCs for 21 days, micro-CT measurements of trabecular bone volume and trabecular thickness were 12% lower than those in the placebo-treated group ($P < 0.05$) (Table 1). Furthermore, the levels of biochemical markers of bone turnover, including osteocalcin, decreased with GC treatment (−16%), while an increase in the level of bone resorption markers, including soluble RANKL (sRANKL) (+44%; $P < 0.05$), TRAP5b (+28%; $P < 0.05$), and DPD (+37%; $P < 0.05$) was observed in GC-treated mice compared with placebo-treated mice (Figure 1A). Compared with placebo treatment, treatment with GCs plus risedronate prevented decreases in trabecular bone volume, trabecular thinning (Figure 1B), and changes in the level of bone turnover

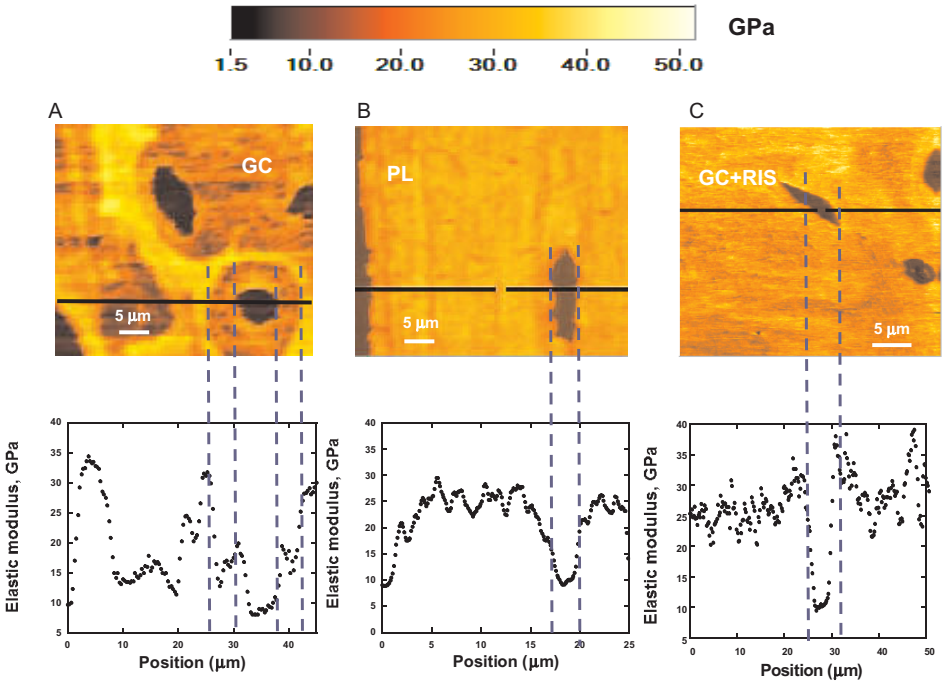

Figure 2. Elastic modulus maps (50×50 μm^2) of an individual trabecula from each of the 3 treatment groups. The false-color scale (from 0 to 50 GPa) is shown above, and line scans corresponding to the horizontal black lines in the maps are shown below. Trabecular bone samples were embedded in methylmethacrylate. **A** and **B,** Areas with a nearly 30% reduction in elastic modulus were observed in the trabeculae of GC-treated mice; such regions were not seen in placebo-treated mice. **C,** Treatment with GCs plus risedronate prevented the reduction in elastic modulus within the trabeculae. See Figure 1 for definitions.

markers (Figure 1A). In addition, treatment with GCs plus risedronate significantly lowered the levels of DPD, sRANKL, and TRAP5b compared with placebo treatment ($P < 0.05$).

Effects of treatment with GCs and risedronate on vertebral bone histomorphometry. Consistent with the micro-CT results, histomorphometric analysis revealed similar reductions in trabecular bone volume and architecture parameters in GC-treated mice compared with placebo-treated animals (data not shown). Tetracycline-based histomorphometry in the GC-treated group showed a reduced rate of mineral apposition (−38%) and surface-based bone formation (−80%), while the osteoclast surface was increased (+112%) in the GC-treated group compared with that in control subjects (all $P < 0.05$) (Table 1). Concurrent treatment of mice with GCs plus risedronate prevented the change in trabecular bone mass and microarchitecture and bone turnover observed in GC-treated mice.

Elastic modulus mapping of trabeculae. Figure 2 shows elastic modulus maps of a trabecula in the fifth lumbar vertebrae from a GC-treated mouse, a placebo-treated mouse, and a mouse treated with GCs plus risedronate. In the color scheme shown, the darker color corresponds to lower values of the locally measured elastic modulus (E). The average number of points tested per trabecula was ~8,700–10,000 and varied with the size of each trabecula. Elastic modulus values were obtained for 3–5 trabeculae per vertebra from each treatment group. The mean ± SD values for the elastic modulus in the GC-treated group and the placebo group were 23.8 ± 3.1 GPa and 24.6 ± 4.4 GPa, respectively (Figures 2A and B), and the mean ± SD value for the elastic modulus in the group receiving GCs plus risedronate was 25.3 ± 4.2 GPa (Figure 2C). The GC-treated mice showed a more prominent reduction in elastic modulus within the trabeculae compared with the groups receiving placebo or GCs plus risedronate (Figure 2). In addition, the GC-treated group showed circular zones or "halos" ~25 μm in radius surrounding a significant number of osteocyte lacunae, with nearly 40% reduced elastic modulus (E ~14 GPa). This marked reduction in elastic modulus surrounding the osteocyte lacunae was not observed in the groups receiving placebo or GCs plus risedronate (Figure 2), indicating that

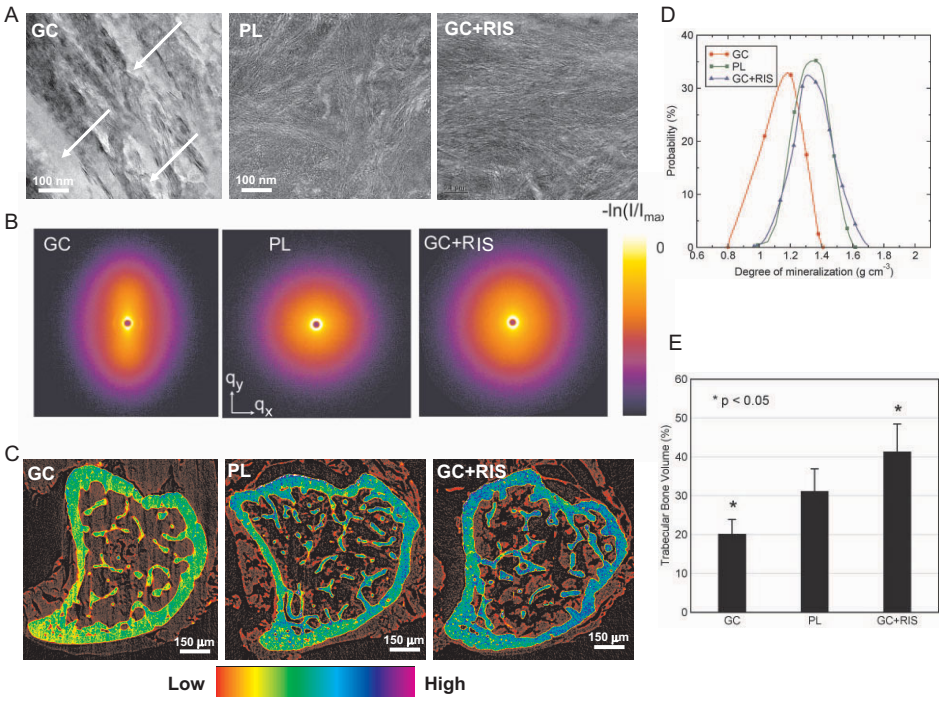

Figure 3. Degree of bone mineralization in mice treated with glucocorticoids (GCs) only and those treated with GCs plus risedronate (RIS). **A,** Transmission electron microscopy micrographs of the trabeculae near an osteocyte lacunae in the groups treated with GCs alone, placebo (PL), or GCs plus risedronate. Note the differences in density and distribution of bone mineral crystals. In particular, submicrometer pockets of lower bone mineral density (**arrows**) were observed exclusively in GC-treated mice. **B,** False-color 2-dimensional images showing results of small-angle x-ray scattering (SAXS) for cortical bone, in the q range $-2\ \text{nm}^{-1} < q_x, q_y < 2\ \text{nm}^{-1}$. The long axis of the bone was oriented parallel to q_x. Azimuthally averaged scattering data were not different between the sample groups, indicating that the mineral crystallite size was not strongly affected by treatment with GCs only or GCs plus risedronate. However, in some measurements from the GC group, one of which is illustrated here, elongation of the SAXS pattern in the q_y direction in the GC data (and the observation of the 67-nm gap diffraction feature in third order) indicates preferential orientation of the mineral crystallites along the bone long axis (34%), while the symmetric patterns for placebo and GCs plus risedronate (8.0% and 4.7%, respectively) revealed a more random crystallite orientation. **C,** X-ray tomography (XTM) of a mouse tibia from each treatment group. The color scale indicates the bone matrix mineral concentration in representative XTM cross-sections. A reduction in the degree of bone mineralization caused by GC treatment was prevented by concurrent treatment with GCs plus risedronate. **D,** Probability distribution of the 3-dimensional degree of mineralization distribution (obtained by XTM from 30 slices below the growth plate of the proximal tibia in secondary spongiosa). The reduction in mineral concentration caused by GC treatment was prevented by concurrent treatment with GCs plus risedronate. **E,** Three-dimensional trabecular bone volume (TBV) of all treatment groups, as assessed by XTM. Concurrent treatment with GCs plus risedronate prevented the GC-induced reduction in TBV. Bars show the mean and SD.

concurrent treatment with risedronate appeared to prevent the localized changes in mechanical properties caused by GC treatment alone.

Transmission electron microscopy (TEM) and SAXS determination of mineral crystal formation. Figure 3A shows typical TEM micrographs of the secondary spongiosa near the osteocyte lacunae in the groups receiving GCs alone, placebo, or GCs plus risedronate. In particular, TEM revealed submicrometer pockets (100–500 nm) of lower BMD in the trabeculae of GC-treated animals (Figure 3A). In mice receiving concurrent treatment with GCs plus risedronate or placebo, TEM revealed fully mineralized bone devoid of pockets of lower BMD, indicating that treatment with GCs plus risedronate prevented this effect (Figure 3A). Therefore, concurrent treatment with GCs plus risedronate appeared to prevent the cessation of individual mineral crystal formation observed in mice treated with GCs alone.

SAXS revealed a difference in a number of locations of crystal thickness and orientation between the GC-treated group and the other groups (Figure 3B). The GC-treated animals had both thicker and more oriented crystallites compared with the groups receiving either placebo or GCs plus risedronate. Therefore, the group receiving placebo and the group receiving GCs

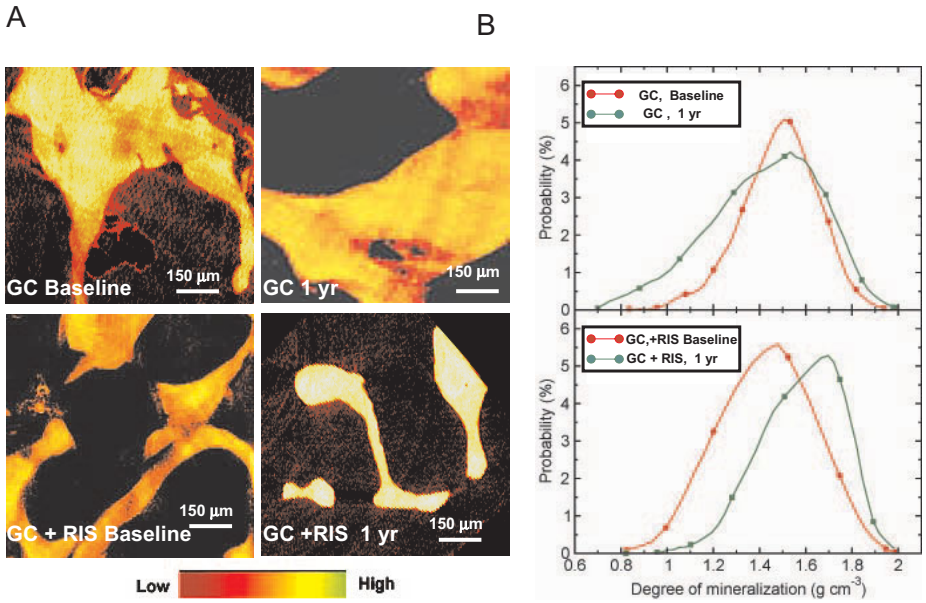

Figure 4. Degree of bone mineralization in human iliac crest biopsy specimens, as assessed by XTM. **A,** Representative XTM cross-sections of human iliac crest biopsy specimens from patients treated with GCs plus placebo or with GCs plus risedronate, at baseline and after 1 year of treatment. Treatment with GCs plus risedronate for 1 year led to an increase in the degree of bone mineralization, compared with treatment with GCs plus placebo. **B,** Distribution of 3-dimensional degree of bone mineralization for each treatment group. The degree of bone mineralization was increased after 1 year of concurrent treatment with GCs and risedronate, while no significant changes between baseline and 1 year were observed in the group receiving GCs plus placebo. See Figure 3 for definitions.

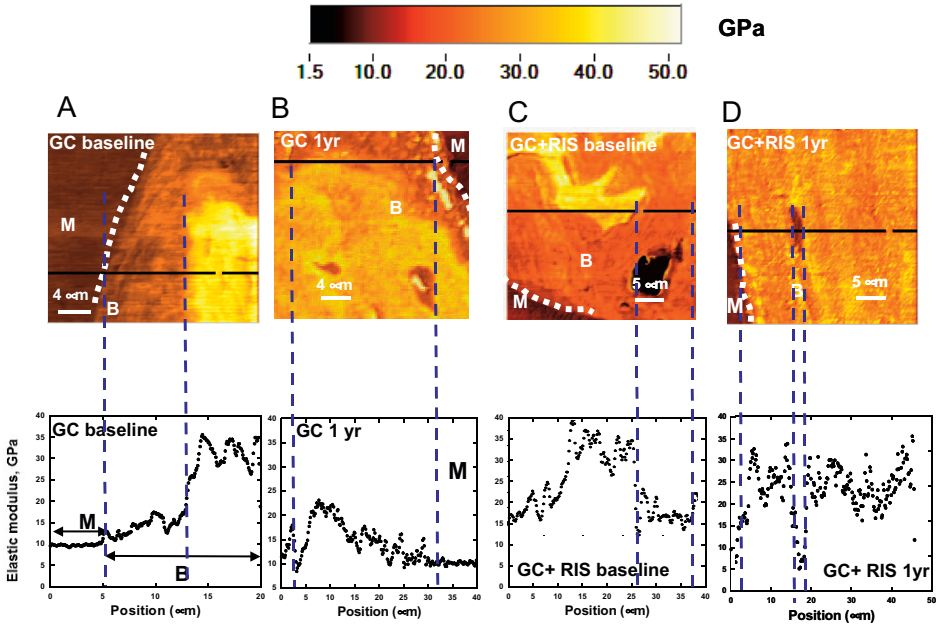

Figure 5. Elastic modulus mapping of human iliac crest biopsy specimens obtained from patients treated with glucocorticoids (GCs) plus placebo (**A** and **B**) or with GCs plus risedronate (RIS) (**C** and **D**), at baseline and after 1 year of treatment. The false-color scale (from 1.5 to 50 GPa) is shown above, and line scans corresponding to the horizontal black lines in the maps are shown below. Dotted white lines indicate the perimeter of the trabeculae proximal to remodeling sites. Concurrent treatment with GCs plus risedronate for 1 year reduced the decreases in elastic modulus near remodeling surfaces that were observed in patients treated with GCs alone. B = trabecular bone; M = methylmethacrylate.

plus risedronate were similar to each other in terms of crystal thickness and orientation, and the group treated with GCs alone was different. TEM showed that bone was well organized in all samples, but there were notable differences in density and distribution of bone mineral.

XTM determination of the degree of mouse bone mineralization. We performed synchrotron XTM of the proximal tibias of each treatment group to determine changes in mineral concentration (Figure 3C), the distribution of the 3-D DBM from multiple slices (Figure 3D), and the BV/TV from multiple slices (Figure 3E). One representative slice from the secondary spongiosa of each group is shown in Figure 3C. Blue and green colors indicate higher mineral concentration, and yellow and red colors indicate lower mineral concentration. There was a significant reduction in mineral concentration in both the cortical and trabecular bone of mice treated with GCs alone compared with the placebo-treated animals (Figure 3C). Furthermore, analysis of 20 slices revealed a 45% reduction in the DBM ($P < 0.001$) and a 14% reduction in the normalized BV/TV ($P < 0.05$) in GC-treated mice compared with placebo-treated mice (Figure 3E). This reduction in the degree of bone mineralization and normalized bone volume was prevented by concurrent treatment with GCs (Figures 3B, D, and E). In fact, concurrent treatment with GCs plus risedronate caused a significant increase in BV/TV compared with that in the placebo-treated group.

XTM of human iliac crest biopsy specimens. Human iliac crest biopsy specimens were evaluated with XTM to determine the effect of a 1-year period of treatment with GCs plus placebo and GCs plus risedronate on the degree of local mineralization in human bone. Iliac crest biopsy specimens were obtained from patients enrolled in a randomized controlled clinical trial, in which all patients receiving GCs were randomized to receive either GCs plus placebo or GCs plus risedronate for 1 year. The biopsy specimens were obtained before treatment (baseline) and after 1 year of treatment (Figure 4A). We observed that patients treated with GCs plus placebo alone had heterogeneity in local mineral concentration, which did not change significantly over the 1 year of the study (Figure 4B). However, the heterogeneity of mineral distribution was reversed over 1 year in patients receiving GCs plus risedronate (Figure 4B). Furthermore, quantification of 3-D DBM values for 300 slices from each group revealed a 32% reduction ($P < 0.01$) in the DBM in patients treated with GCs plus placebo compared with patients treated with GCs plus risedronate for 1 year (Figure 4B). Treatment with GCs plus placebo for 1 year did not lead to a statistically significant reduction in the average DBM; however, the distribution of DBM values appeared to be more heterogeneous than that observed in the other treatment groups.

Elastic modulus mapping of human iliac crest biopsy specimens. To determine whether changes in the DBM with GC treatment, as shown by XTM of human bone (Figures 4A and B), are coupled with changes in local material properties, elastic modulus mapping of human iliac crest biopsy specimens was performed by atomic force microscopy–nanoindentation. Baseline biopsy specimens from patients treated with GCs plus placebo alone showed a reduction in local elastic modulus, E, at the perimeter of the trabeculae near remodeling sites (Figure 5A), which appeared more pronounced after an additional year of treatment with GCs plus placebo (Figure 5B). After 1 year of treatment with GCs plus risedronate, however, there was essentially no reduction in local elastic modulus near remodeling sites (Figures 5C and D).

Biomechanical findings. Compression testing of the sixth lumbar vertebrae (Figures 6A and B) of mice in each treatment group was conducted to determine changes in macromechanical properties, specifically the compressive stiffness and strength. Results indicated that on day 21, the sixth lumbar vertebrae of mice treated with GCs had a 14% reduction in strength ($P < 0.05$) and a 21% reduction in compression modulus ($P < 0.05$) compared with placebo-treated mice. However, the sixth lumbar vertebrae of mice treated with GCs plus risedronate had a 40% increase in strength ($P < 0.01$), a 64% increase in the compression modulus ($P < 0.001$), and a 40% increase in stiffness ($P < 0.01$), compared with placebo-treated mice (Figures 6A and B).

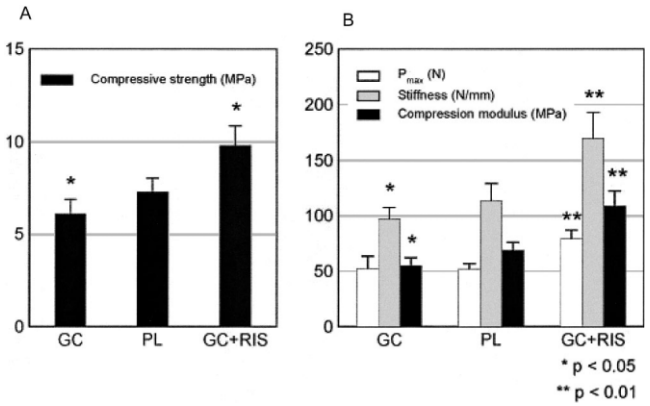

Figure 6. Biomechanical properties of the sixth lumbar vertebral bodies of mice treated with GCs plus risedronate (n = 8), placebo (PL; n = 6), or GCs alone (n = 6). **A,** Compressive strength. **B,** Compressive stiffness. Animals treated with GCs plus risedronate had a significant elevation in all measured mechanical property parameters, as compared with the group receiving placebo and the group receiving GCs alone. Bars show the mean and SD. See Figure 5 for other definitions.

DISCUSSION

Aminobisphosphonates are frequently prescribed for the prevention and treatment of GC-induced bone loss and other metabolic diseases of bone that have high bone turnover as a main feature. However, the mechanism by which these agents reduce fracture risk is still unknown, because the increases in bone mass after bisphosphonate treatment, as evaluated by BMD, can account for only a small part of the reduction in fracture risk (4–7). Previously, our group reported that the bones of mice treated with GCs had changes in localized mechanical properties and matrix composition at the surface of trabecular bone and around the osteocyte lacunae (20). Furthermore, we determined that similar reductions in localized elastic modulus and the degree of mineralization were present in both humans and mice treated with GCs. Concurrent treatment with GCs plus risedronate also appeared to prevent changes in the elastic modulus, the degree of bone mineralization, and whole bone compression strength observed with GCs alone.

In the present study, we demonstrated that GC treatment reduced the degree of trabecular bone mineralization in mice and in clinical biopsy specimens, which, from a mechanical properties perspective, translated into a bone matrix structure with localized regions of much lower elastic modulus. Treatment with GCs lowers osteoblast activity, which reduces the mineralizing surface and bone formation rates described in histomorphometric analyses (18,20). The lower mineral concentrations resulting from GC treatment may be secondary to reduced formation of osteoid. Also, GCs have been reported to be antiapoptotic and prolong survival of osteoclasts, while other investigators reported that GCs suppressed osteoclast activity in in vitro and in vivo studies (18,31). Therefore, the reduced osteoblast activity and prolonged survival of osteoclasts, either separately or together, may shorten the secondary mineralization phase of the bone remodeling cycle and reduce mineralization (32,33). Treatment with GCs plus risedronate not only prevented the loss of trabecular bone mineralization, but modestly increased it.

Postmenopausal women with osteoporosis treated with risedronate were reported to have reduced activation frequency by histomorphometric analysis, and an increased secondary mineralization phase of the bone remodeling cycle which together might explain the increased mineralization (9,32,33). Iliac crest biopsy specimens from postmenopausal women treated with bisphosphonates were reported to have larger crystal size, higher mineral-to-matrix ratios, and more uniformity of the mineralized bone matrix compared with untreated control subjects (32,33). Estrogen treatment of postmenopausal women also increased bone mineralization of the iliac crest, with increased ratios of high-to-low mineral (33), but this effect was less than what has been observed in patients treated with bisphosphonates. Ibandronate increased crystal size, the mineral-to-matrix ratio, and uniformity of the mineralized bone matrix in beagle dogs (34). Tiludronate treatment of ovariectomized rats increased only crystal width without altering the crystal length or other characteristics (35). The observation of reduced fracture risk in patients treated with GCs and either risedronate or alendronate and preservation of localized material properties and compression strength in mice suggests that the changes in the degree of bone mineralization may be associated with improved localized material properties of the bone in individuals treated with these agents.

Elastic modulus mapping of the trabecular surface of both GC-treated mice and GC-treated patients revealed regions of reduced elastic modulus within the trabeculae as well as at the remodeling surface. The reduced elastic modulus at the trabecular surface may be attributable to a GC-induced increase in the number of osteoclasts and reduced osteoblast activity, which together would reduce the level of localized bone mineral (20); concurrent treatment with risedronate prevented this in mice. The reduced elastic modulus surrounding the osteocyte lacunae in mice treated with GCs for 21 days resulted in a lower mineral-to-matrix ratio, as assessed by micro-Raman spectroscopy (18,20). The mechanism of risedronate for maintenance of the elastic modulus around the osteocyte lacunae is not clear. It is known that GC treatment leads to increased osteocyte apoptosis (18); however, this may be dependent on the dose of GCs and the duration of GC therapy. Possibly, concurrent treatment with risedronate plus GCs prevented apoptosis, which may then prevent the localized changes in mineralization and elastic modulus. In vitro studies of treatment with GCs plus risedronate are needed to evaluate the effects on osteocyte metabolism.

Although most bisphosphonates in clinical use appear to prevent GIOP and reduce incident fractures in patients treated concurrently with both agents, the mechanism for this is still unclear. Treatment with bisphosphonates in the presence of GCs appears to reduce bone turnover, most likely by reducing osteoclast activity and/or life span, and this may prevent the loss of bone mineral and maintain bone strength. In addition, the interaction of these agents with hydroxyapatite crys-

tals may also explain improvements in bone strength. Bisphosphonates bind to hydroxyapatite and inhibit mineral dissolution. There are differences in kinetic binding affinities and hydroxyapatite crystal growth with the bisphosphonates, due to differences in their side chain moieties, where zoledronic acid and alendronate appear more potent than risedronate and etidronate (19). The differences in binding of these agents to hydroxyapatite may contribute to their uptake and retention in bone. The interaction of risedronate and GCs with crystals is beyond the scope of this study. However, additional experiments will allow us to determine how risedronate and other bisphosphonates alter bone matrix properties.

The ability of risedronate to prevent deterioration of the degree of bone mineralization and hence the local mechanical properties, defined at nano/microscale dimensions, in GC-treated mice reiterates the importance of local mechanical properties and bone matrix composition in determining stiffness, strength, and toughness, which govern the fracture risk in bone. Measuring bone matrix mechanical properties and composition with high spatial resolution permits the understanding of how risedronate treatment affects mineral crystal formation and orientation, the degree of local bone mineralization, and the mechanical properties of trabecular bone near important areas, such as remodeling sites and osteocyte lacunae. Exactly how risedronate treatment leads to reduced bone fragility, and whether these effects are dose dependent, remain unclear; however, the prevention of localized reductions in modulus and the degree of mineralization in GC-treated patients and mice, while not detected with BMD measurements, can have definitive effects on crack initiation and propagation and, ultimately, bone toughness. Whereas whole bone density and bone macroarchitecture remain important parameters in understanding the effect of bisphosphonates on bone integrity, our study has shown that local nanoscale properties, structure and composition of the bone matrix near remodeling sites, and osteocyte lacunae should also be considered when studying current and future therapeutic interventions for bone fragility caused by metabolic diseases of bone.

Although our study has many strengths, including the measurement of the trabecular bone at nanoscale levels and the evaluation of the effects of GCs on both mouse and human bone, it also has several weaknesses. We tested only 1 low-to-moderate dose of GCs, and the study duration was only 21 days; therefore, the results may not be generalizable to higher doses of GCs or studies in which GC treatment is of longer duration. Also, because this study was undertaken to determine whether GCs plus risedronate could prevent GC-induced changes to the bone matrix, we did not include a positive control group of animals treated with risedronate; thus, we cannot speculate whether any of the effects we observed in this model of treatment with GCs plus risedronate would also be present in normal bone. We had only a small number of iliac crest bone biopsy specimens from subjects in the GIOP study who received GCs plus placebo or GCs plus risedronate for 1 year, and it may not be appropriate to generalize these results to either the entire study group or to other studies of chronic GIOP (36). Also, it should be appreciated that elastic modulus mapping and SAXS are local measurement techniques that assess behavior over very small dimensions on small amounts of bone tissue. These results are important, because they provide information on structure and properties at nanoscale to microscale dimensions; however, additional correlation analyses of the properties of whole bone material are still needed.

In conclusion, this study demonstrated that treatment with GCs plus risedronate prevented the deterioration of trabecular bone volume, microarchitecture, and localized material properties of bone that is observed with GC treatment alone. These results expand our knowledge about how aminobisphosphonates prevent GC-induced bone loss and fractures. Additional work is now required to determine the mechanism by which aminobisphosphonates prevent GC-induced changes in bone mineralization and bone strength.

ACKNOWLEDGMENTS

We thank Dr. Roger Phipps (Proctor & Gamble Pharmaceuticals) for supplying the iliac crest biopsy samples and Fred M. Tileston, Jr. for careful editing of the manuscript.

AUTHOR CONTRIBUTIONS

Dr. Lane had full access to all of the data in the study and takes responsibility for the integrity of the data and the accuracy of the data analysis.

Study design. Yao, Lane.

Acquisition of data. G. Balooch, Yao, Ager, M. Balooch, Nalla, Ritchie, Lane.

Analysis and interpretation of data. Yao, Ager, M. Balooch, Ritchie, Lane.

Manuscript preparation. Yao, Ager, Ritchie, Lane.

Statistical analysis. Yao, Ager, Lane.

ROLE OF THE STUDY SPONSOR

Proctor and Gamble had no role in the study design or in the collection, analysis, or interpretation of the data.

REFERENCES

1. Cooper C, Coupland C, Mitchell M. Rheumatoid arthritis, corticosteroid therapy and hip fracture. Ann Rheum Dis 1995;54:49–52.
2. Lane NE. An update on glucocorticoid-induced osteoporosis [review]. Rheum Dis Clin North Am 2001;27:235–53.
3. Saag KG. Glucocorticoid-induced osteoporosis [review]. Endocrinol Metab Clin North Am 2003;32:135–57, vii.
4. Delaney MF, Hurwitz S, Shaw J, LeBoff MS. Bone density changes with once weekly risedronate in postmenopausal women. J Clin Densitom 2006;6:45–50.
5. Adachi JD, Bensen WG, Brown J, Hanley D, Hodsman A, Josse R, et al. Intermittent etidronate therapy to prevent corticosteroid-induced osteoporosis. N Engl J Med 1997;337:382–7.
6. Eastell R, Barton I, Hannon RA, Chines A, Garnero P, Delmas PD. Relationship of early changes in bone resorption to the reduction in fracture risk with risedronate. J Bone Miner Res 2003;18:1051–6.
7. Saag KG, Emkey R, Schnitzer TJ, Brown JP, Hawkins F, Goemaere S, et al, for the Glucocorticoid-Induced Osteoporosis Intervention Study Group. Alendronate for the prevention and treatment of glucocorticoid-induced osteoporosis. N Engl J Med 1998;339:292–9.
8. Bauer DC, Black DM, Garnero P, Hochberg M, Ott S, Orloff J, et al. Change in bone turnover and hip, non-spine, and vertebral fracture in alendronate-treated women: the Fracture Intervention Trial. J Bone Miner Res 2004;19:1250–8.
9. Cohen S, Levy RM, Keller M, Boling E, Emkey RD, Greenwald M, et al. Risedronate therapy prevents corticosteroid-induced bone loss: a twelve-month, multicenter, randomized, double-blind, placebo-controlled, parallel-group study. Arthritis Rheum 1999; 42:2309–18.
10. Wallach S, Cohen S, Reid DM, Hughes RA, Hosking DJ, Laan RF, et al. Effects of risedronate treatment on bone density and vertebral fracture in patients on corticosteroid therapy. Calcif Tissue Int 2000;67:277–85.
11. Boutsen Y, Jamart J, Esselinckx W, Devogelaer JP. Primary prevention of glucocorticoid-induced osteoporosis with intravenous pamidronate and calcium: a prospective controlled 1-year study comparing a single infusion, an infusion given once every 3 months, and calcium alone. J Bone Miner Res 2001;16: 104–12.
12. Eastell R, Devogelaer JP, Peel NF, Chines AA, Bax DE, Sacco-Gibson N, et al. Prevention of bone loss with risedronate in glucocorticoid-treated rheumatoid arthritis patients. Osteoporos Int 2000;11:331–7.
13. Coxon FP, Helfrich MH, Van't Hof R, Sebti S, Ralston SH, Hamilton A, et al. Protein geranylgeranylation is required for osteoclast formation, function, and survival: inhibition by bisphosphonates and GGTI-298. J Bone Miner Res 2000;15:1467–76.
14. Luckman SP, Hughes DE, Coxon FP, Graham R, Russell G, Rogers MJ. Nitrogen-containing bisphosphonates inhibit the mevalonate pathway and prevent post-translational prenylation of GTP-binding proteins, including Ras. J Bone Miner Res 1998;13: 581–9.
15. Reszka AA, Halasy-Nagy JM, Masarachia PJ, Rodan GA. Bisphosphonates act directly on the osteoclast to induce caspase cleavage of mst1 kinase during apoptosis: a link between inhibition of the mevalonate pathway and regulation of an apoptosis-promoting kinase. J Biol Chem 1999;274:34967–73.
16. Asahi H, Mizokami A, Miwa S, Keller ET, Koshida K, Namiki M. Bisphosphonate induces apoptosis and inhibits pro-osteoclastic gene expression in prostate cancer cells. Int J Urol 2006;13: 593–600.
17. Plotkin LI, Weinstein RS, Parfitt AM, Roberson PK, Manolagas SC, Bellido T. Prevention of osteocyte and osteoblast apoptosis by bisphosphonates and calcitonin. J Clin Invest 1999; 104:1363–74.
18. Weinstein RS, Chen JR, Powers CC, Stewart SA, Landes RD, Bellido T, et al. Promotion of osteoclast survival and antagonism of bisphosphonate-induced osteoclast apoptosis by glucocorticoids. J Clin Invest 2002;109:1041–8.
19. Nancollas GH, Tang R, Phipps RJ, Henneman Z, Gulde S, Wu W, et al. Novel insights into actions of bisphosphonates on bone: differences in interactions with hydroxyapatite. Bone 2006;38: 617–27.
20. Lane NE, Yao W, Balooch M, Nalla RK, Balooch G, Habelitz S, et al. Glucocorticoid-treated mice have localized changes in trabecular bone material properties and osteocyte lacunar size that are not observed in placebo-treated or estrogen-deficient mice. J Bone Miner Res 2006;21:466–76.
21. Yao W, Balooch G, Balooch M, Jiang Y, Nalla RK, Kinney J, et al. Sequential treatment of ovariectomized mice with bFGF and risedronate restored trabecular bone microarchitecture and mineralization. Bone 2006;39:460–9.
22. Yao W, Hadi T, Jiang Y, Lotz J, Wronski TJ, Lane NE. Basic fibroblast growth factor improves trabecular bone connectivity and bone strength in the lumbar vertebral body of osteopenic rats. Osteoporos Int 2005;16:1939–47.
23. Kinney JH, Haupt DL, Balooch M, Ladd AJ, Ryaby JT, Lane NE. Three-dimensional morphometry of the L6 vertebra in the ovariectomized rat model of osteoporosis: biomechanical implications. J Bone Miner Res 2000;15:1981–91.
24. Parfitt AM. Bone histomorphometry: standardization of nomenclature, symbols and units (summary of proposed system). Bone 1988;9:67–9.
25. Parfitt AM, Drezner MK, Glorieux FH, Kanis JA, Malluche H, Meunier PJ, et al. Bone histomorphometry: standardization of nomenclature, symbols, and units. Report of the ASBMR Histomorphometry Nomenclature Committee. J Bone Miner Res 1987; 2:595–610.
26. Balooch G, Marshall GW, Marshall SJ, Warren OL, Asif SA, Balooch M. Evaluation of a new modulus mapping technique to investigate microstructural features of human teeth. J Biomech 2004;37:1223–32.
27. Engqvist H, Botton GA, Couillard M, Mohammadi S, Malmstrom J, Emanuelsson L, et al. A novel tool for high-resolution transmission electron microscopy of intact interfaces between bone and metallic implants. J Biomed Mater Res A 2006;78:20–4.
28. Porter AE, Buckland T, Hing K, Best SM, Bonfield W. The structure of the bond between bone and porous silicon-substituted hydroxyapatite bioceramic implants. J Biomed Mater Res A 2006;78:25–33.
29. Fratzl P, Schreiber S, Klaushofer K. Bone mineralization as studied by small-angle x-ray scattering. Connect Tissue Res 1996; 34:247–54.
30. Akhter MP, Cullen DM, Gong G, Recker RR. Bone biomechanical properties in prostaglandin EP1 and EP2 knockout mice. Bone 2001;29:121–5.
31. Kim HJ, Zhao H, Kitaura H, Bhattacharyya S, Brewer JA, Muglia LJ, et al. Glucocorticoids suppress bone formation via the osteoclast. J Clin Invest 2006;116:2152–60.
32. Borah B, Dufresne TE, Ritman EL, Jorgensen SM, Liu S, Chmielewski PA, et al. Long-term risedronate treatment normalizes mineralization and continues to preserve trabecular architecture: sequential triple biopsy studies with micro-computed tomography. Bone 2006;39:345–52.
33. Faibish D, Ott SM, Boskey AL. Mineral changes in osteoporosis: a review. Clin Orthop Relat Res 2006;443:28–38.

34. Monier-Faugere MC, Geng Z, Paschalis EP, Qi Q, Arnala I, Bauss F, et al. Intermittent and continuous administration of the bisphosphonate ibandronate in ovariohysterectomized beagle dogs: effects on bone morphometry and mineral properties. J Bone Miner Res 1999;14:1768–78.
35. Rohanizadeh R, LeGeros RZ, Bohic S, Pilet P, Barbier A, Daculsi G. Ultrastructural properties of bone mineral of control and tiludronate-treated osteoporotic rat. Calcif Tissue Int 2000;67: 330–6.
36. Chavassiuex PM, Arlot ME, Roux JP, Portero N, Daifotis A, Yates J, et al. Effects of alendronate on bone quality and remodeling in glucocorticoid-induced osteoporosis: a histomorphometric analysis of transiliac biopsies. J Bone Miner Res 2000;15:754–62.